PHYSICAL REVIEW A VOLUME 4, NUMBER 3 SEPTEMBER 1971

Elastic and Inelastic Scattering of Protons by Hydrogen Atoms*

Victor Franco
Physics Department and Institute for Nuclear Theory,
Brooklyn College of the City University of New York, Brooklyn, New York 11210

and

Brian K. Thomas
Department of Physics, University of Pittsburgh, Pittsburgh, Pennsylvania 15213
(Received 12 February 1971)

The Glauber approximation is applied to elastic scattering of protons by hydrogen atoms and to excitation of the $2s$, $2p$, $3s$, and $3p$ levels of the hydrogen atom by proton impact. The predicted differential and integrated elastic and excitation cross sections are compared with other calculations and with the available experimental data. A minimum appears in both the $1s$-$2s$ and $1s$-$3s$ integrated cross sections near 15 keV. The corresponding differential cross sections near 15 keV exhibit a minimum and a maximum at very small scattering angles. The Glauber approximation is a considerable improvement over the Born approximation at energies $<\sim 200$ keV and the distortion approximation at energies $<\sim 100$ keV. At energies $>\sim 200$ keV, our calculated total excitation cross sections are close to the Born approximation. Nevertheless, over most of the angular range our calculated differential cross sections are very different from the Born-approximation values. Above 10 keV our results are in good agreement with the only available experimental data ($1s$-$2p$), indicating that above ~ 10 keV the Glauber approximation should yield reasonable estimates for proton–hydrogen-atom collision cross sections.

I. INTRODUCTION

Scattering approximations are perhaps best tested by applying them to systems whose internal structure and interaction with the incident projectile are both known. In recent years one of the most successful methods for describing medium- and high-energy nuclear collisions has been the Glauber approximation.[1] Applications of this approximation to nuclear scattering problems generally require a knowledge of hadron-nucleon interactions and of the structure of the nucleus, both of which are imperfectly known. These difficulties are avoided, however, by applying the approximation to scattering of charged particles by hydrogen atoms or other simple atomic systems. In such applications the internal structure of the scattering system is usually well known as is the interaction between the incident particle and the system. Thus applications to atomic scattering may be the most stringent tests of collision theories. The possibility of using atomic systems as testing grounds for scattering theories is, in itself, both convenient and of interest. Furthermore the application of the Glauber approximation to atomic scattering is of additional significance since its region of applicability covers an energy range for which the Born approximation is inaccurate, and most other approximations are either inaccurate or prohibitively tedious.

The Glauber approximation for atomic collisions was first described by Franco[2] for scattering of charged particles by hydrogen atoms with particular applications to elastic scattering of electrons by ground-state hydrogen. Subsequently Tai *et al.*[3] and Ghosh *et al.*[4] analyzed inelastic scattering of electrons by ground-state hydrogen. The theory was also extended to scattering of charged particles by helium atoms[5] with particular applications to elastic scattering of electrons by ground-state helium and to scattering by arbitrary atoms.[5] The applications to scattering by hydrogen showed that below 200 eV the Glauber approximation yielded integrated cross sections which were in good agreement with measurements, whereas the first Born approximation gave results which compared poorly with the data. Above 200 eV, where the first Born approximation might be expected to be accurate, the integrated cross sections from the Glauber and Born approximations were nearly identical. Nevertheless, the two approximations revealed very different *differential* cross sections, even above 200 eV. A similar conclusion was found in the application to elastic scattering by helium. The existing data showed[3,5,6] that the differential cross sections obtained from the Glauber approximation were in rather good agreement with the measurements, whereas those obtained from the first Born approximation, particularly at small angles in the elastic scattering collisions and at large angles in the inelastic scattering processes, were not. Thus the Glauber approximation has been particularly successful in describing electron scattering above 200 eV, where the Born approxi-

mation is still not very accurate and, perhaps more significantly, at energies even as low as approximately 30 eV, where the Born approximation is very poor. It appears, therefore, that intermediate- and high-energy scattering of electrons by atomic hydrogen is now reasonably well described.

The relative success of the Glauber approximation analyses of electron scattering leads naturally to the question of its applicability to the scattering of protons. We present here the theory and calculations for elastic and inelastic scattering of protons by ground-state atomic hydrogen, together with comparisons with existing measurements. Scattering of protons by atomic hydrogen is potentially more complex than scattering of electrons since for a given incident velocity a proton can transfer a very much greater momentum to the target than can an electron. Furthermore, the minimum velocity required by protons to effect inelastic transitions is much smaller than that required by electrons. In addition, near the velocities which correspond to threshold for electron scattering, incident protons can effect the transitions with approximately half the momentum transfer needed in electron collisions. These properties of proton collisions, including the great increase in the range of the physically allowed momentum transfers, in both the small and large momentum transfer regions, could (and, as we shall see, indeed do) give rise to effects which are absent in electron-hydrogen collisions. Furthermore, the scattering of protons by atomic hydrogen is perhaps of greater fundamental interest and complexity than the scattering of electrons because of the presence of additional reaction channels corresponding to charge transfer (proton-proton exchange is negligible except at extremely high energies). In the first Born approximation, coupling between reaction channels is completely ignored. The impact-parameter form of the close-coupling approximation, which is already nontrivial, is made considerably more complicated by the addition of the charge-transfer channels. In fact, all approximations which hope to explicitly include the effects of coupling suffer much the same fate when charge-transfer states are included. On the other hand, the Glauber approximation implicitly contains coupling to all states of the system. These states do not explicitly appear in the resulting equations of the Glauber approximation since they are eliminated by means of a closure approximation. Presumably the Glauber approximation, therefore, would contain the effects of coupling not only to the direct but also to the charge-transfer reaction channels.

In our analysis we consider the direct reactions

$$H^+ + H(1s) \rightarrow H^+ + H(1s, 2s, 2p, 3s, 3p) \quad (1)$$

for incident protons with kinetic energies greater than approximately 1 keV. In Secs. II and III we briefly describe the Glauber approximation for scattering by hydrogen atoms and present the theoretical expressions for the scattering amplitudes and cross sections for the various inelastic and elastic collision processes. In Sec. IV we present our results and compare them with other theories and the existing experimental data.

II. SCATTERING AMPLITUDES

We consider a spinless structureless particle of mass m and charge Z incident upon a hydrogen atom of mass M initially at rest. Let $\vec{K}_i$ and $\vec{K}_f$ be the initial and final momenta, respectively, of the incident particle in the center-of-mass system. In terms of the initial and final relative velocities we have $\hbar\vec{K}_i = \mu\vec{v}_i$ and $\hbar\vec{K}_f = \mu\vec{v}_f$, where $\mu = mM/(m+M)$. Of course, since the hydrogen atom is initially at rest, $\vec{v}_i$ is just the velocity of the incident particle in the laboratory. Let $\vec{q}$ be the momentum-transfer vector defined by

$$\vec{q} = \vec{K}_i - \vec{K}_f \ .$$

The Glauber approximation amplitudes for scattering in which the atom undergoes a transition from an initial state i to a final state f are given by

$$F_{fi}(\vec{q}) = (iK_i/2\pi) \int u_f^*(\vec{r})\, \Gamma(\vec{b}, \vec{r})\, u_i(\vec{r})\, e^{i\vec{q}\cdot\vec{b}}\, d^2b\, d\vec{r} \ , \quad (2)$$

where u_i and u_f are the initial and final bound-state wave functions of the atom,

$$\Gamma(\vec{b}, \vec{r}) = 1 - e^{i\chi(\vec{b}, \vec{r})} \ , \quad (3)$$

and the phase-shift function χ is given by

$$\chi(\vec{b}, \vec{r}) = -(1/\hbar v_i) \int_{-\infty}^{\infty} V(\vec{b}, \vec{r}; \zeta)\, d\zeta \ . \quad (4)$$

In Eq. (4), $V(\vec{b}, \vec{r}; \zeta)$ is the potential seen by the incident particle. We neglect spin-dependent interactions so that V is just the sum of Coulomb potentials between the incident particle and the atomic target.

In the above equations, $\vec{r}'$ and $\vec{r}$ denote the coordinates, of the incident particle and the bound electron, respectively, relative to the atom nucleus; we have written $\vec{r}' = \vec{b} + \vec{\zeta}$, where $\hat{\zeta}$ is the direction (in the center-of-mass system) of the path of integration in Eq. (4) and $\vec{b}$ is the projection of $\vec{r}'$ onto the plane perpendicular to $\hat{\zeta}$. Furthermore, in Eq. (2) it is assumed that the vector $\vec{q}$ is perpendicular to $\hat{\zeta}$, i.e., that $\vec{q}$ lies in the plane containing $\vec{b}$. For intermediate- and high-energy incident protons (kinetic energies > 10 keV) the major portion of the scattering will be into small angles *near* the forward direction, so that to good approximation the vector $\vec{q}$ is nearly per-

pendicular to $\vec{K}_i$, $\vec{b}$ is the impact parameter vector in the center-of-mass system, and $\hat{\xi}$ is approximately in the direction of $\vec{K}_i$.

For particles of charge Z incident upon atomic hydrogen, Eq. (3) becomes[2]

$$\chi(\vec{b}, \vec{r}) = 2n \ln(|\vec{b} - \vec{s}|/b) , \tag{5}$$

where

$$n = -Ze^2/\hbar v_i \tag{6}$$

and $\vec{s}$ is the projection of $\vec{r}$ onto the plane containing $\vec{b}$, i.e., perpendicular to $\hat{\xi}$.

The amplitudes of Eq. (2) corresponding to the transitions of Eq. (1) have been evaluated by Franco[2] and by Tai *et al.*[3] for incident electrons. With the understanding that $\hbar\vec{K}_i$ is the initial momentum of the incident particle in the center-of-mass system and n is given by Eq. (6), these results are applicable in general to particles of arbitrary mass and charge. For completeness we present here the results which we shall apply to proton-hydrogen scattering. The bound-state wave functions are quantized along the direction $\hat{\xi}$, and the amplitudes are expressed in atomic units.

The amplitudes for the transitions $1s \to 1s$, $2s$, $3s$ are given by

$$F_{1s,1s}(\vec{q}) = 2iK_i \int_0^{\pi/2} \sin^3\theta\cos\theta \, \frac{(\sin^2\theta - \frac{1}{2}q^2\cos^2\theta)}{(\sin^2\theta + \frac{1}{4}q^2\cos^2\theta)^4} \, \gamma_0(n, \theta)\, d\theta , \tag{7}$$

$$F_{2s,1s}(\vec{q}) = \frac{-2^{10}\sqrt{2}}{3^6} iK_i \int_0^{\pi/2} \sin^3\theta\cos\theta \, \frac{(\sin^4\theta - \frac{28}{9}q^2\cos^2\theta\sin^2\theta + \frac{64}{81}q^4\cos^4\theta)}{(\sin^2\theta + \frac{4}{9}q^2\cos^2\theta)^5} \, \gamma_0(n, \theta)\, d\theta , \tag{8}$$

$$F_{3s,1s}(\vec{q}) = \frac{-3^3\sqrt{3}}{2^6} iK_i \int_0^{\pi/2} \frac{[\sin^6\theta + \frac{9}{8}q^2\cos^2\theta\sin^4\theta - (3^7/2^8)q^4\cos^4\theta\sin^2\theta + (3^7/2^{10})q^6\cos^6\theta]}{(\sin^2\theta + \frac{9}{16}q^2\cos^2\theta)^6} \times \sin^3\theta\cos\theta\, \gamma_0(n, \theta)\, d\theta , \tag{9}$$

where

$$\gamma_0(n, \theta) = 1 - (1/\pi)(\cos\theta)^{-2in} \int_0^{\pi} (1 - \sin2\theta\cos\phi)^{in} d\phi . \tag{10}$$

The integral in Eq. (10) may be evaluated from the previously used[2] formula

$$(1/\pi) \int_0^{\pi} (1 - \sin2\theta\cos\phi)^{in} d\phi = |\cos2\theta|^{1+2in} {}_2F_1(\tfrac{1}{2} + \tfrac{1}{2}in, 1 + \tfrac{1}{2}in; 1; \sin^2 2\theta), \tag{11}$$

so that Eq. (10) becomes[7]

$$\gamma_0(n, \theta) = 1 - (\cos\theta)^{-2in} |\cos2\theta|^{1+2in} \times {}_2F_1(\tfrac{1}{2} + \tfrac{1}{2}in, 1 + \tfrac{1}{2}in; 1; \sin^2 2\theta). \tag{12}$$

For the transitions $1s \to 2p$, $3p$, the amplitudes depend upon the orbital magnetic quantum number m of the final bound state. When $m = 0$ we have

$$F_{2p_0,1s}(\vec{q}) = F_{3p_0,1s}(\vec{q}) = 0 , \tag{13}$$

and when $m = \pm 1$ we have

$$F_{2p_{\pm1},1s}(\vec{q}) = e^{\mp i\phi_q} \frac{2^{12}}{3^6} K_i q \times \int_0^{\pi/2} \sin^4\theta\cos^2\theta \, \frac{(\sin^2\theta - \frac{4}{9}q^2\cos^2\theta)}{(\sin^2\theta + \frac{4}{9}q^2\cos^2\theta)^5} \, \gamma_1(n, \theta)\, d\theta , \tag{14}$$

$$F_{3p_{\pm1},1s}(\vec{q}) = e^{\mp i\phi_q} \frac{3^5}{2^8} K_i q \int_0^{\pi/2} \sin^4\theta\cos^2\theta \times \frac{[\sin^4\theta + \frac{27}{4}q^2\sin^2\theta\cos^2\theta - (3^6/2^8)q^4\cos^4\theta]}{(\sin^2\theta + \frac{9}{16}q^2\cos^2\theta)^6} \times \gamma_1(n, \theta)\, d\theta , \tag{15}$$

where

$$\gamma_1(n, \theta) = (1/\pi)(\cos\theta)^{-2in} \int_0^{\pi} \cos\phi\,(1 - \sin2\theta\cos\phi)^{in} d\phi \tag{16}$$

or[3,8]

$$\gamma_1(n, \theta) = -\tfrac{1}{2}in(\cos\theta)^{-2in}\sin2\theta\,|\cos2\theta|^{1+2in} \times {}_2F_1(1 + \tfrac{1}{2}in, \tfrac{3}{2} + \tfrac{1}{2}in; 2; \sin^2 2\theta) . \tag{17}$$

In these results $\phi_q - \pi$ is the azimuthal scattering angle. This completes the specification of the Glauber approximation amplitudes.

III. CROSS SECTIONS

We may obtain the differential cross section in the center-of-mass system from the scattering amplitudes by means of the relation

$$\frac{d\sigma_{fi}}{d\Omega} = \frac{K_f}{K_i} |F_{fi}(\vec{q})|^2 , \tag{18}$$

where $d\Omega$ is the element of solid angle in the center-

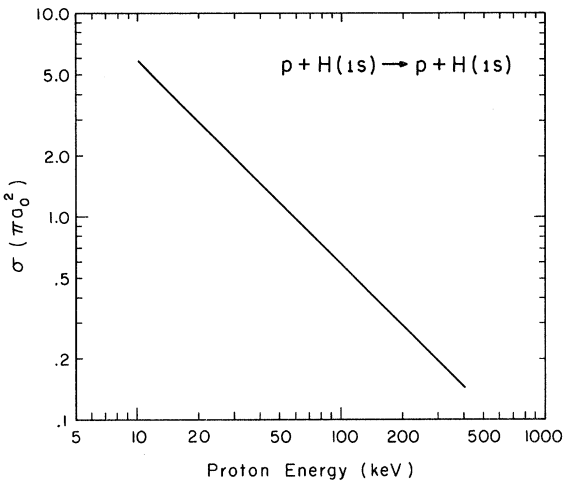

FIG. 1. Integrated elastic scattering cross section, in units of πa_0^2, for protons incident upon atomic hydrogen as a function of the laboratory kinetic energy. The straight line represents both the Glauber and first Born approximations, which are nearly identical over the energy range shown.

of-mass system. Furthermore K_f is determined by

$$K_f^2 = K_i^2 - (2\mu/\hbar^2)(\epsilon_f - \epsilon_i) ,$$

where ϵ_i and ϵ_f are the energies of the initial and final bound states.

The integrated cross section may be written as

$$\sigma_{fi} = (K_f/K_i) \int |F_{fi}(\vec{q})|^2 d\Omega . \tag{19}$$

If we take advantage of the fact that

$$q^2 = K_i^2 + K_f^2 - 2K_i K_f \cos\theta , \tag{20}$$

where θ is the scattering angle in the center-of-mass system, the integrated cross section becomes

$$\sigma_{fi} = (1/K_i^2) \int_{K_i-K_f}^{K_i+K_f} q\, dq \int_0^{2\pi} |F_{fi}(\vec{q})|^2 d\phi_q . \tag{21}$$

The amplitudes given by Eqs. (7)–(9), (14), and (15) are such that $|F_{fi}|^2$ is azimuthally symmetric. The functions $|F_{fi}|^2$ depend only on the magnitude of $\vec{q}$, not on its orientation. Consequently we have

$$\sigma_{fi} = (2\pi/K_i^2) \int_{K_i-K_f}^{K_i+K_f} |F_{fi}(q)|^2 q\, dq . \tag{22}$$

IV. RESULTS AND DISCUSSION

We have calculated the amplitudes and cross sections of Secs. II and III for incident protons with laboratory energies E such that $1 < E \leq 400$ keV. The amplitudes were computed by numerically integrating Eqs. (7)–(9), (14), and (15) at a sufficient number of the physically allowed values of q to enable a determination of the integrated cross section $\sigma_{fi}(E)$ to within an accuracy of 1%. The hypergeometric functions appearing in γ_0 and γ_1 were computed via their relatively simple integral representations and also via their power-series expansions. The integrated cross sections were then computed by means of Eq. (22).

A. Elastic Scattering

In Fig. 1 the Glauber approximation for the integrated elastic scattering cross section is shown as a function of the laboratory kinetic energy of the incident proton. In the energy region shown the cross section is equal, to three significant figures, to that obtained from the first Born approximation. The curve in Fig. 1 is, in fact, a straight line, reflecting the E^{-1} dependence of both predictions.[9] For $E \geq 10$ keV we have

$$\sigma_{\text{elastic}}^{\text{Born}}(E) \approx \sigma_{\text{elastic}}^{\text{Glauber}}(E) \approx 58/E \text{ (keV) (in units of } \pi a_0^2). \tag{23}$$

The virtual equality of the cross sections obtained from the two approximations over such a large energy range is a rather surprising result, particularly in view of Fig. 2, which shows the center-of-mass differential cross section (in units of πa_0^2) as a function of q. The solid curves are the Glauber approximation for 15- and 200-keV protons. The dashed curve is the first Born approximation, which is the same function of q for all energies. As $q \to 0$ the Glauber curves diverge[2] as $\ln^2 q$, whereas the first Born curve approaches $\mu^2/\pi \approx M^2/4\pi$. As $q \to \infty$ both curves fall off as q^{-4}. The asymptotic behavior of the Glauber elastic amplitudes for

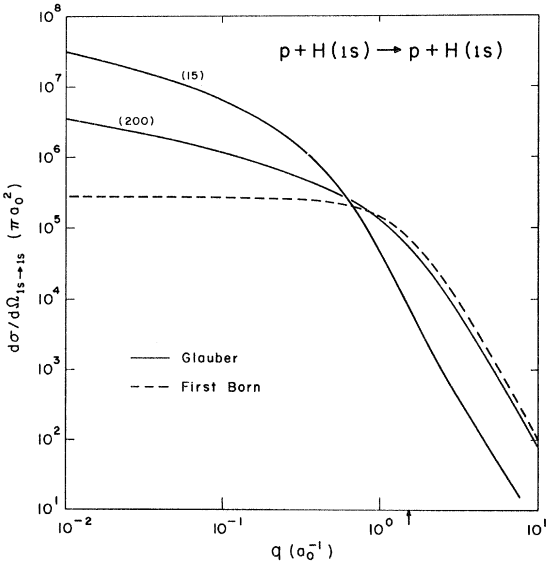

FIG. 2. Center-of-mass differential cross section, in units of πa_0^2, as a function of the momentum transfer q, in units of a_0^{-1}, for 15- and 200-keV protons elastically scattered by atomic hydrogen. The solid curves are the Glauber approximation; the dashed curve is the first Born approximation.

large q is not easily obtained from Eqs. (7) and (12). However, Thomas and Gerjuoy[10] have recently obtained closed-form expressions for the Glauber amplitudes which require no further integration. Taking the limit of large q in their expression for the elastic amplitude, one obtains the above result. Alternatively, one may expand the hypergeometric function appearing in Eq. (12) in a series which converges everywhere within the range of integration[7] and integrate term by term. One obtains an infinite series of hypergeometric functions with delicate convergence properties for arbitrary q. However, by using an appropriate analytic continuation for these hypergeometric functions when q is large, one can show that the leading term in the expansion of the amplitude in powers of q^{-1} is, in fact, proportional to q^{-2} and therefore $|F|^2 \propto q^{-4}$.

Since the integrated cross sections obtained from the two approximations are nearly identical, the integral in Eq. (22) has virtually the same value for each curve in Fig. 2. The differences between the Glauber and Born curves therefore cancel exactly, or almost exactly.

Since the Glauber amplitudes are nontrivial functions of the speed of the incident particle, it is not possible, short of explicitly computing the amplitudes and cross sections, to determine easily the proton energies at which the Glauber and first Born total elastic cross sections begin to differ significantly. Although the equality of the Born and Glauber integrated elastic cross sections occurs in electron-hydrogen scattering above 100 eV, it does not occur, for example, for incident electrons with the same velocity as 15-keV protons. The reason for this difference results from the very unequal momentum transfer ranges physically available in the two cases. For 15-keV protons the upper limit in the cross-section integral (22) is

$$q_{\max} = 2K_i \approx 1.42 \times 10^3 a_0^{-1} .$$

The energy of an electron with the same velocity as a 15-keV proton is 8.2 eV. As we can see from Fig. 1 of Ref. 2, the Glauber integrated cross section exceeds the Born cross section by almost a factor of 2 for such an electron. The corresponding electron-hydrogen differential cross sections as a function of q are given by the 15-keV curve of Fig. 2 of the present work, provided the curve is reduced by a factor of $(\frac{1}{2}M)^2$. Now, however, the upper limit in the integrated cross-section integral is only $q_{\max} \approx 1.55\ a_0^{-1}$, as indicated by the arrow on the q scale of Fig. 2. It is this small value for the upper limit which leads to the large difference between the Glauber and Born predictions of the integrated cross section for such an electron.

It is worth noting that the Glauber differential cross sections for protons with kinetic energies of 184 keV, 920 keV, and 9.2 MeV may be obtained directly from Fig. 2 of Ref. 2 by multiplying the cross sections given by those curves by the factor $(\frac{1}{2}M)^2$.

B. Inelastic Scattering

In Fig. 3 we compare our calculation of the integrated direct $1s$-$2s$ excitation cross section (curve G) with various other theoretical predictions. Curve B is the first Born approximation,[11] curve D is the distortion approximation of Bates,[12] and curve F is the close-coupling result of Flannery.[13] Curves D and F were calculated from the impact parameter form of the close-coupling approximation. The distortion approximation assumes that only the coupling between the initial and final atom bound states is significant, whereas Flannery has included coupling to the $1s$, $2s$, and $2p_{0,\pm1}$ direct reaction channels.

The integrated $1s$-$2s$ cross sections obtained from the Glauber approximation lie well below those obtained from the Born approximation at energies less than ~100 keV. This is expected since a similar relationship between the two approximations exists for the $1s$-$2s$ cross sections in electron-hydrogen collisions.[3] The Glauber approximation differs qualitatively from all the other calculations shown in Fig. 3 by the presence of a minimum near 15 keV.[14] One effect of the appearance of this minimum is to shift the kinematical maximum to higher energies and to exhibit an additional maximum near 8 keV. Above 150 keV the Glauber and distortion approximations are essentially indistinguishable. The Flannery curve lies everywhere above the Born curve for energies greater

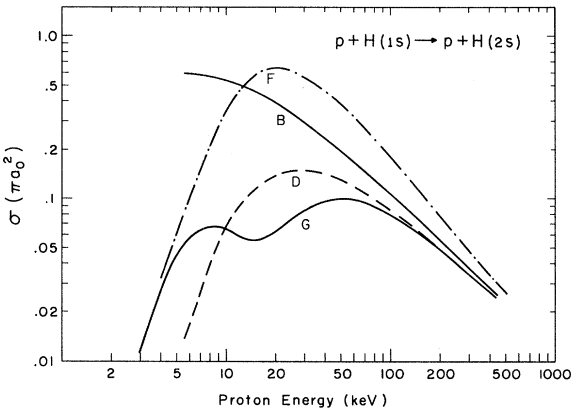

FIG. 3. Integrated cross section in units of πa_0^2, for the $1s$-$2s$ excitation of atomic hydrogen by proton impact, as a function of the laboratory kinetic energy of the proton. Curve G is the Glauber approximation; curve B is the first Born approximation (Ref. 11); curve F is the close-coupling calculation of Flannery (Ref. 13); curve D is the distortion approximation of Bates (Ref. 12).

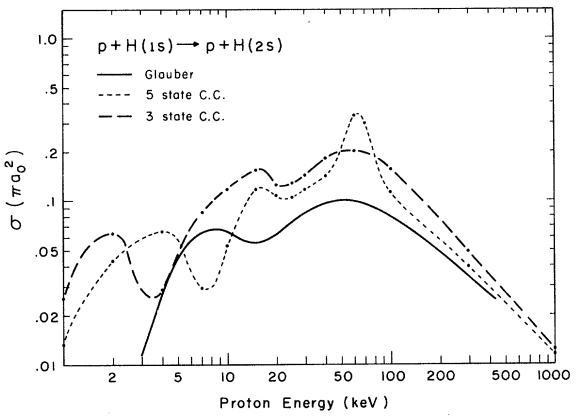

FIG. 4. Integrated cross section for $1s$-$2s$ excitation. The solid curve is the Glauber approximation. The two dashed curves are the 3- and 5-state close-coupling results of Ref. 17. The solid circles represent the values actually calculated in Ref. 17.

than 12 keV, presumably because of the inclusion of the optically allowed $1s$-$2p$ channel and the strong long-range $2s$-$2p$ dipole coupling. Flannery has recently repeated his calculation, [15] but now also includes the influence of all ion-multipole interactions with the ground state. The inclusion of the pseudostates defined by these interactions raises curve F everywhere by a factor ranging from approximately 60% at low incident proton energies to approximately 20% at high energies. However, it is quite probable that both of Flannery's results overestimate the $1s$-$2s$ cross section near his maximum (~ 20 keV) since coupling to charge-transfer states is not included in those calculations. At 20 keV, where the maximum of curve F occurs, the cross section for charge transfer into the $2s$ state, as measured by Bayfield, [16] is approximately $0.4\ \pi a_0^2$ which is of the same order of magnitude as the cross section of curve F at that energy. It is reasonable to at least assume, therefore, that resonant coupling between the final direct and charge-transfer channels may be strong and therefore should not be ignored. It is interesting to note that the minimum in the Glauber curve roughly coincides with the maximum of the $2s$ charge-transfer cross section.

In Fig. 4 we compare our total cross sections (solid curve) for $1s$-$2s$ direct excitation with the recent and rather arduous close-coupling calculations of Cheshire, Gallaher, and Taylor. [17] The results of Cheshire *et al.* were obtained from the impact parameter form of the close-coupling approximation in which coupling with the charge-transfer channels was included. In particular, the "3-state" close-coupling results (long-dashed curve) were obtained by explicitly coupling to the $1s$, $2s$, and $2p$ states of hydrogen in both the direct and charge-transfer channels. The "5-state" results (short-dashed curve) were obtained by adding pseudostates to the previous set of states. These pseudostates, which we designate by $(3s)'$ and $(3p)'$, were constructed with energies corresponding, respectively, to the $n = 1$ and $n = 2$ states of atomic hydrogen but orthogonal to them. In this manner a 99% overlap with the first three states of He^+ was achieved. Furthermore, the $(3s)'$ state lies almost entirely in the hydrogen continuum whereas the $(3p)'$ states overlap the complete set of hydrogen bound states by 86%. Again, these states were included in both the direct and charge-transfer channels. The solid circles on the close-coupling curves of Fig. 4 are the actual cross-section values computed by Cheshire *et al.*

By comparing curve F of Fig. 3 with the "3-state" result of Fig. 4, we see that for $1s$-$2s$ excitation inclusion of the charge-transfer states reduces the Flannery result by a factor of ~ 3 near 20 keV, as expected. However, beyond 200 keV the two curves are almost identical, reflecting the fact that including the charge-transfer states does not appreciably affect the long-range $2s$-$2p$ dipole coupling in the direct channel. Aside from enhancing the primary maximum near 60 keV, the inclusion of the $(3s)'$ and $(3p)'$ pseudostates lowers the cross section everywhere beyond 10 keV. Beyond 100 keV the "5-state" curve is indistinguishable from the first Born curve of Fig. 3, so that at high energies the effect of coupling to the pseudostates is to cancel that of the direct dipole coupling. Furthermore, beyond 5 keV we note a striking similarity in the gross over-all structure of the close-coupling curves and the Glauber approximation.

Although the two close-coupling curves are not consistent with one another below 10 keV, they both predict a third maximum in the cross section between 1 and 5 keV which does not appear in the Glauber curve. However, if the Glauber curve were extended to lower energies, a third maximum would appear just below 1 keV, but with a cross section which is only of the order of $10^{-3}\ \pi a_0^2$. At present there exist no experimental data for the $1s$-$2s$ excitation with which to compare the theoretical predictions. The structure in the $1s$-$2s$ Glauber curve for proton impact was not observed for incident electrons[3] primarily because an electron having a velocity equal to that of a 5- or 10-keV proton cannot induce the $1s$-$2s$ transition.

The anomalous behavior of the Glauber integrated $1s$-$2s$ cross section between 5 and 25 keV is reflected in the differential cross sections of Fig. 5, which shows the center-of-mass differential cross sections for direct excitation to the $2s$ state as functions of the momentum transfer q. The

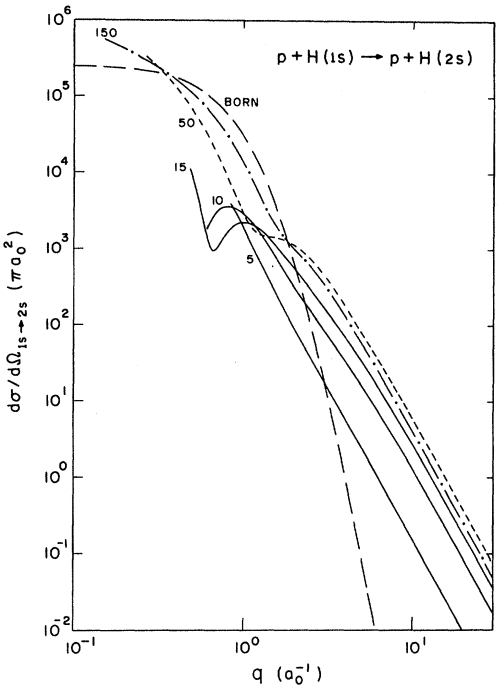

FIG. 5. Center-of-mass differential cross section for the $1s$-$2s$ transition, as a function of the momentum transfer q. The long-dashed curve is the first Born approximation (Ref. 11), which is independent of incident energy. The other curves are the Glauber predictions for 5-, 10-, 15-, 50-, and 150-keV protons.

long-dashed curve is the first Born approximation,[11] which is independent of the incident proton energy. The other curves are the Glauber predictions for 5-, 10-, 15-, 50-, and 150-keV protons. The left end point of each of these curves corresponds to scattering in the forward direction. Since at these proton energies $K_i^2 \gg 2\mu(\epsilon_{2s}-\epsilon_{1s})/\hbar^2$ and therefore $K_f/K_i \approx 1$, the curves of Fig. 5 are just the absolute squares of the scattering amplitudes as a function of q for the energies shown.

We can now see how the minimum in the Glauber integrated cross section occurs. For example, in order for the integrated cross section at 15 keV to be *greater* than that at 10 keV, $\int(d\sigma/d\Omega)q\,dq$ at 15 keV would have to be *greater than* 1.5 *times* the corresponding integral at 10 keV [see Eq. (22)]. It is seen in Fig. 5 that for $q > 1.3a_0^{-1}$ the intensity for the $1s$-$2s$ transition is somewhat greater for 15-keV protons than for 10-keV protons. However, for 15-keV protons the differential cross-section possesses a rather deep minimum in a momentum transfer region where the intensity for 10-keV protons contributes substantially to the total integrated cross section. This rather large decrease of the intensity for 15-keV protons below that for 10-keV protons is not sufficiently compensated for by the larger intensity for 15-keV protons in the large-q region, since the intensities in that region rapidly become too small to contribute appreciably to the total integrated cross section. Nor does the additional small-q range physically available to 15-keV protons, but not to 10-keV protons, sufficiently compensate the effect of the minimum; this additional range is quite small and, furthermore, occurs for $q < 1$ so that the extra factor of q in the integrand of Eq. (22) tends to minimize the contribution of this range to the integral. Thus although the integral $\int(d\sigma/d\Omega)q\,dq$ at 15 keV *is* indeed greater than the integral at 10 keV, the minimum in the intensity for 15-keV protons is deep and broad enough and occurs over an important momentum transfer range so that, together with the kinematical factor K_i^{-2} in Eq. (22), it is sufficient to produce a minimum in the integrated cross section. If regarded simply as functions of q and extended to the left, the Glauber curves of Fig. 5 diverge as $\ln^2 q$ as q approaches zero, in contrast to the Born curve which approaches a finite value. For large q the Glauber curves fall off as q^{-4} (Ref. 10), whereas the Born approximation goes to zero as q^{-12} (Ref. 11). The large-q behavior of the Glauber $1s$-$2s$ amplitude reflects the fact that the contribution to the Glauber inelastic amplitudes arising from the proton-nucleus interaction does not vanish as it does in Born approximation. We also note a rather curious behavior of the Glauber curves with varying incident particle energy, but fixed large q. Namely, the 150-keV curve lies everywhere between the 15- and 50-keV curves for $q > 2a_0^{-1}$. Again, the energy dependence of the $1s$-$2s$ amplitude is not easily extracted from Eq. (8). However, from Ref. 10 we see that for large q

$$|F_{2s,1s}|^2 \propto (\pi n/\sinh\pi n)^2 n^2(1+n^2)\,, \tag{24}$$

where n is defined by Eq. (6). Hence at fixed large q, $d\sigma_{2s,1s}/d\Omega \to 0$ as $E \to 0$ and decreases as $E \to \infty$.

We might note that the shoulder in $d\sigma/d\Omega$ at 50 keV may be viewed as a precursor to the minimum in $d\sigma/d\Omega$ at the lower energy of 15 keV. It is interesting to note that a shoulder also exists in $d\sigma/d\Omega$ for $1s$-$2s$ transitions in *electron*-hydrogen scattering at 50 eV (see Fig. 8 of Ref. 3). It would not surprise us to find a minimum at lower energies in electron-hydrogen scattering unless the energy at which it would be expected to occur was below 10.2 eV, the excitation energy for the $2s$ state, or unless the momentum transfer at which it would be expected to occur was below the minimum momentum transfer physically allowed at that energy.

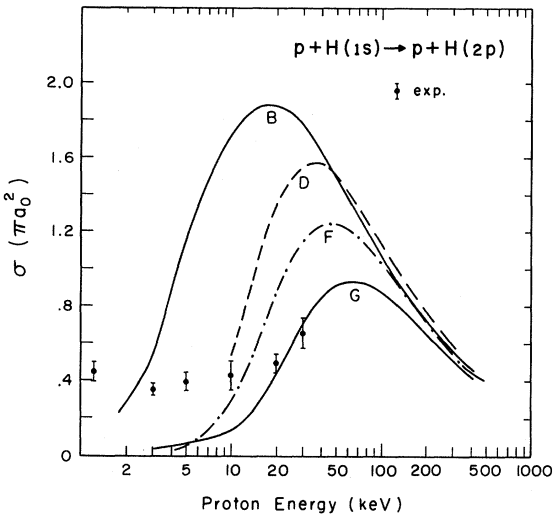

FIG. 6. Integrated cross section for $1s$-$2p$ excitation by proton impact, as a function of proton laboratory kinetic energy. Curve G is the Glauber approximation; curve B is the first Born approximation (Ref. 11); curve D is the distortion approximation (Ref. 18); curve F is the close-coupling calculation of Flannery (Ref. 13). The experimental results are by Stebbings *et al.* (Ref. 19).

In Fig. 6 we compare the Glauber $1s$-$2p$ excitation cross section (curve G) with the predictions of the various theoretical approximations previously discussed. Curves B, D, and F correspond to the same Born,[11] distortion,[18] and close-coupling[13] approximations used in the curves of Fig. 3. The experimental values were measured by Stebbings *et al.*[19] Again the Glauber approximation lies well below the first Born approximation at energies less than 100 keV. Above 30 keV the distortion approximation (curve D) lies very close to the Born approximation, indicating that distortion is less important for $1s$-$2p$ excitation than for $1s$-$2s$ excitation, a point which has been fully discussed by Bates.[18] The inclusion of back coupling to the direct $2s$ reaction channel in the close-coupling calculations of Flannery (curve F) now acts to reduce the cross section. We note that of the calculations shown in Fig. 6, the Glauber approximation is the only one which reproduces the experimental values above 10 keV. We also note that the minimum present in the Glauber approximation for the $1s$-$2s$ integrated cross section does not appear in the $1s$-$2p$ cross section above 3 keV.

In Fig. 7 we compare the Glauber integrated cross section (solid curve) for $1s$-$2p$ direct excitation with the recent close-coupling calculation of Ref. 17 discussed earlier. As in Fig. 4, the solid circles on the close-coupling curves are the actual values computed by Cheshire *et al.* In Fig. 7 we see that the effect of the charge-transfer channels in $1s$-$2p$ excitation is not as great as in $1s$-$2s$ excitation. Between 20 and 100 keV the "3-state" close-coupling curve of Cheshire *et al.* lies only ~ 30% below curve F of Fig. 6. Now, however, the main effect of the pseudostates is to enhance the primary maximum of the cross section. We note that above 10 keV the Glauber approximation does as well as, if not somewhat better than, either of the close-coupling results in predicting the experimental results. Below 10 keV the close-coupling approximation predicts a second maximum in the cross section, whereas the Glauber appears to go smoothly to zero with decreasing energy.

The Glauber approximation differential cross sections for the direct excitation of the $2p$ states of hydrogen are compared in Fig. 8 with the first Born approximation which is independent of the incident proton energy. The Glauber predictions are shown for proton energies of 5, 20, 50, and 150 keV, and the left end point of each of those curves corresponds to scattering in the forward direction. If we formally let q approach zero in the Glauber and Born expressions for the differential cross section, we find that in both approximations the differential cross section diverges as q^{-2}, reflecting the fact that the $1s$-$2p$ transition is dipole allowed. As q gets large the Glauber approximation differential cross section becomes proportional to q^{-6} (Ref. 10) whereas the Born-approximation differential cross section falls off as q^{-14} (Ref. 11). The Glauber curves display none of the minima or maxima evident at low energies in the differential cross sections shown in Fig. 5. The differential

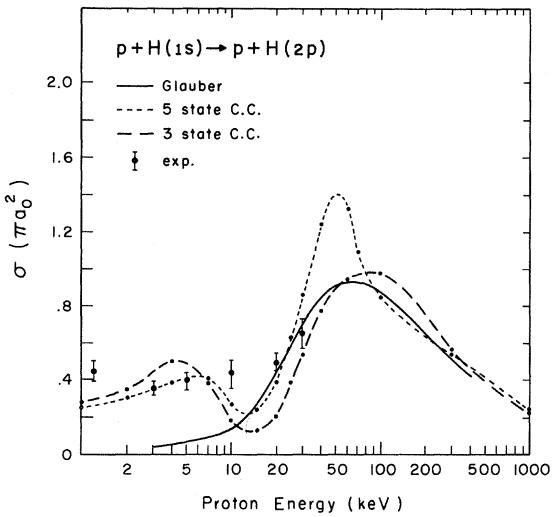

FIG. 7. Integrated Glauber cross section for $1s$-$2p$ excitation is compared with the results of Cheshire *et al.* (Ref. 17). The curves are as in Fig. 4. The experimental results are by Stebbings *et al.* (Ref. 19).

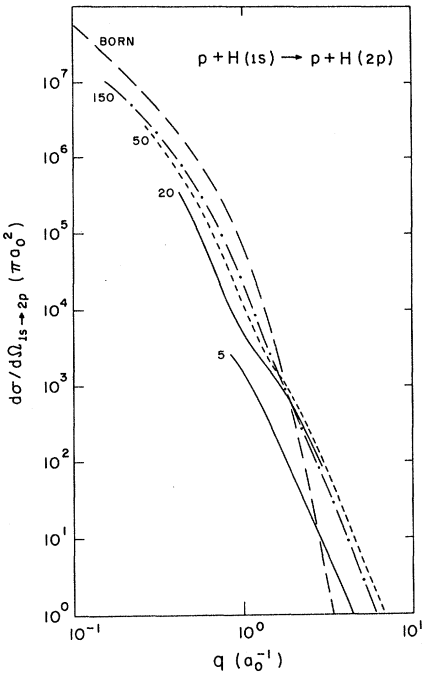

FIG. 8. Center-of-mass differential cross section for $1s$-$2p$ excitation, as a function of the momentum transfer q. The long-dashed curve is the first Born approximation (Ref. 11), which is independent of incident energy. The other curves are the Glauber predictions for 5-, 20-, 50-, and 150-keV protons.

cross sections are now monotonically decreasing with increasing q in the energy range we have investigated. The behavior of the cross sections as functions of the incident energy at fixed large q is[10]

$$|F_{2p,1s}|^2 \propto (\pi n/\sinh\pi n)^2 n^2 (1+n^2)^2 . \quad (25)$$

In Fig. 9 we show our integrated cross sections for the $1s$-$3s$ and $1s$-$3p$ excitations of atomic hydrogen by proton impact, and compare the results with the first Born approximation.[11] The relations between the Glauber and Born curves are much the same as were observed in Figs. 2 and 5, including the presence of a minimum in the Glauber $1s$-$3s$ cross section near 15 keV. Both the $1s$-$3s$ and the $1s$-$3p$ cross sections attain their kinematical maximum near 60 keV in the Glauber approximation. The $1s$-$3p$ cross section decreases more rapidly with decreasing energy than does the $1s$-$3s$ cross section.

Byron[20] has recently derived the Glauber approximation from the close-coupling approximation by coupling to a complete set of atom states (complete in the sense that the closure approximation is accurate) under certain kinematical conditions including

$$K_i a_0 \gg 1 \quad (26)$$

and

$$a_0 \Delta E/\hbar v_i \ll 1 , \quad (27)$$

where a_0 is the Bohr radius and ΔE is a typical energy difference occurring in the problem. When Eq. (26) holds and the energy of the incident particle is much greater than the average strength of the potential, Byron obtains what is essentially the impact-parameter form of the close-coupling approximation. Then using Eq. (27) he obtains the Glauber approximation. The first condition is easily understood, and apparent in all other derivations of the Glauber approximation.[1] However, the second condition could be surprisingly stringent. It is equivalent to the restriction that the speed of the incident particle be large compared with the speed of the bound electron, a condition generally assumed in most derivations of the Glauber approximation.

In view of the preceding remarks, the comparisons in Figs. 4 and 7 are not so surprising. It is also clear why the Glauber approximation is a considerable improvement over the results of Flannery. The work of Cheshire *et al.* confirms, as one might well expect, that if in the close-coupling approximation one couples to a finite number of states, those states corresponding to charge transfer should be explicitly included. However, in the Glauber approximation we are already

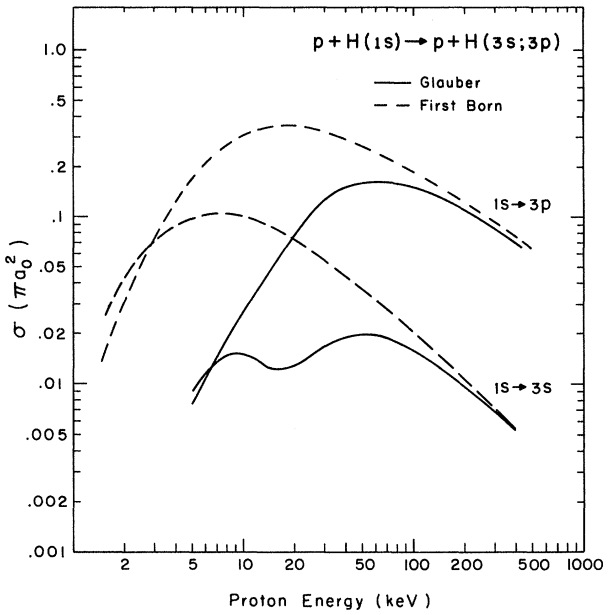

FIG. 9. $1s$-$3s$ and $1s$-$3p$ excitation cross sections as functions of the proton laboratory kinetic energy. The solid curves are the Glauber predictions. The dashed curves are the results of the first Born approximation (Ref. 11).

coupling to a *complete set* of atom states in the direct channels so that the use of additional charge-transfer states would be redundant, i.e., the set of basis states would be over-complete. In other words, the set of charge-transfer states is already included in the Glauber approximation. Furthermore, the results of Byron imply that as an increasing number of states are included in the close-coupling approximation, the results should converge to the Glauber approximation, provided both Eqs. (26) and (27) are satisfied, i.e., at proton energies greater than at least 100 keV. This convergence is in fact indicated by Figs. 4 and 7. We can also better understand why the Glauber approximation fails for proton energies less than 5 keV. Of course condition (26) is satisfied. However, since the velocity of a 5 keV proton is only approximately 0.45 a.u., the condition (27) is not satisfied for any bound-bound transition from the ground state of atomic hydrogen. The rapid decrease of the $1s$-$2s$ integrated cross section below 5 keV may be interpreted in terms of this failure. Furthermore, the absence of a maximum in the Glauber $1s$-$2p$ cross section between 1 and 10 keV might be attributed to competition between the processes leading to such a maximum and the rapid breakdown of Eq. (27).

In general we have seen that the Glauber approximation for proton-hydrogen scattering yields results consistent with those obtained for electron-hydrogen scattering. At proton energies below 100 keV but greater than 5 keV the Glauber approximation is most certainly a distinct improvement over either of the Born or distortion approximations. Furthermore, the similarities between the Glauber results and those obtained from the impact-parameter form of the close-coupling approximation can be explained in terms of the work by Byron. Hence we concluded that for proton energies above approximately 10 keV the Glauber approximation should provide quite reasonable estimates of the proton–hydrogen-atom collision cross sections.

ACKNOWLEDGMENT

We wish to thank Professor E. Gerjuoy for suggesting this problem.

---

*Work supported in part by the National Science Foundation under Grant No. GP-16913 at Brooklyn College, by the CUNY Faculty Research Program under Grant Nos. 1122 and 1344 at Brooklyn College, by the Advanced Research Projects Agency under Contract No. DA-31-124-ARO-D-440, and by the National Aeronautics and Space Administration under Contract NGL-39-011-035, at the University of Pittsburgh.

[1]R. J. Glauber, in *Lectures in Theoretical Physics*, Vol. 1, edited by W. E. Brittin *et al.* (Interscience, New York, 1959), p. 315.

[2]V. Franco, Phys. Rev. Letters 20, 709 (1968).

[3]H. Tai, R. H. Bassel, E. Gerjuoy, and V. Franco, Phys. Rev. A 1, 1819 (1970).

[4]A. S. Ghosh, P. Sinha, and N. C. Sil, J. Phys. B 3, L58 (1970).

[5]V. Franco, Phys. Rev. A 1, 1705 (1970); Phys. Rev. Letters 26, 1088 (1971).

[6]H. Tai, P. J. Teubner, and R. H. Bassel, Phys. Rev. Letters 22, 1415 (1969); 23, 453(E) (1969).

[7]The hypergeometric function can be further reduced by applying a standard linear transformation [*Handbook of Mathematical Functions*, edited by M. Abromowitz and I. P. Stegun (U.S. GPO, Washington, D.C., 1965), p. 559]. One finds that

$$\gamma_0(n, \Theta) = 1 - (\cos\Theta)^{-2in}\,{}_2F_1(\tfrac{1}{2} - \tfrac{1}{2}in, -\tfrac{1}{2}in;\ 1;\ \sin^2 2\Theta).$$

If one is going to compute γ_0 from a series expansion, the above expression has the advantage that the standard series for the hypergeometric function converges for all values of $\sin^2 2\theta$ when θ is real.

[8]The comments of Ref. 7 again apply, only now

$$\gamma_1(n, \theta) = -\tfrac{1}{2}in(\cos\theta)^{-2in}(\sin 2\theta)\,{}_2F_1(1 - \tfrac{1}{2}in, \tfrac{1}{2} - \tfrac{1}{2}in;\ 2,\ \sin^2 2\theta).$$

[9]The same E^{-1} dependence in the Glauber approximation occurs in elastic electron-hydrogen scattering. See Ref. 2.

[10]B. K. Thomas and E. Gerjuoy, J. Math. Phys. (to be published).

[11]D. R. Bates and G. Griffing, Proc. Phys. Soc. (London) 67, 961 (1953).

[12]D. R. Bates, Proc. Phys. Soc. (London) 73, 227 (1959).

[13]M. R. Flannery, J. Phys. B 2, 1044 (1969).

[14]V. Franco and B. K. Thomas, Bull. Am. Phys. Soc. 15, 1504 (1970).

[15]M. R. Flannery, J. Phys. B 3, 1083 (1970).

[16]J. E. Bayfield, Phys. Rev. 185, 105 (1969).

[17]I. M. Cheshire, D. F. Gallaher, and A. J. Taylor, J. Phys. B 3, 813 (1970).

[18]D. R. Bates, Proc. Phys. Soc. (London) 77, 59 (1961).

[19]R. F. Stebbings, R. A. Young, C. L. Oxley, and E. Ehrhardt, Phys. Rev. 138, A1312 (1964).

[20]F. W. Byron, Jr., Phys. Rev. (to be published).